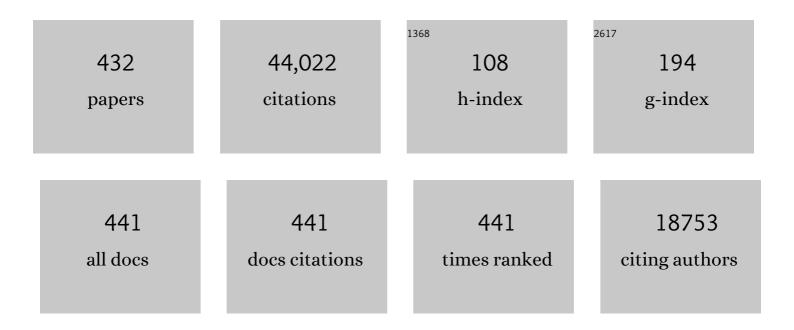
Harald Ade

List of Publications by Year in descending order

Source: https://exaly.com/author-pdf/3283030/publications.pdf Version: 2024-02-01



Ηλρλιή Δηε

#	Article	IF	CITATIONS
1	Resolving the Molecular Origin of Mechanical Relaxations in Donor–Acceptor Polymer Semiconductors. Advanced Functional Materials, 2022, 32, 2105597.	7.8	15
2	Introducing Lowâ€Cost Pyrazine Unit into Terpolymer Enables Highâ€Performance Polymer Solar Cells with Efficiency of 18.23%. Advanced Functional Materials, 2022, 32, 2109271.	7.8	49
3	Understanding, quantifying, and controlling the molecular ordering of semiconducting polymers: from novices to experts and amorphous to perfect crystals. Materials Horizons, 2022, 9, 577-606.	6.4	117
4	High Miscibility Compatible with Ordered Molecular Packing Enables an Excellent Efficiency of 16.2% in All‧mallâ€Molecule Organic Solar Cells. Advanced Materials, 2022, 34, e2106316.	11.1	74
5	Semi-paracrystallinity in semi-conducting polymers. Materials Horizons, 2022, 9, 1196-1206.	6.4	18
6	Conjugated polymers with controllable interfacial order and energetics enable tunable heterojunctions in organic and colloidal quantum dot photovoltaics. Journal of Materials Chemistry A, 2022, 10, 1788-1801.	5.2	6
7	Organic solar powered greenhouse performance optimization and global economic opportunity. Energy and Environmental Science, 2022, 15, 1659-1671.	15.6	26
8	Branched Alkoxy Side Chain Enables High-Performance Non-Fullerene Acceptors with High Open-Circuit Voltage and Highly Ordered Molecular Packing. Chemistry of Materials, 2022, 34, 2059-2068.	3.2	20
9	16.52% Efficiency Allâ€Polymer Solar Cells with High Tolerance of the Photoactive Layer Thickness. Advanced Materials, 2022, 34, e2108749.	11.1	63
10	Low Voltageâ€Loss Organic Solar Cells Light the Way for Efficient Semitransparent Photovoltaics. Solar Rrl, 2022, 6, .	3.1	3
11	Ultrathin P(NDI2ODâ€T2) Films with High Electron Mobility in Both Bottomâ€Gate and Topâ€Gate Transistors. Advanced Electronic Materials, 2022, 8, .	2.6	7
12	Optimizing spectral and morphological match of nonfullerene acceptors toward efficient indoor organic photovoltaics with enhanced light source adaptability. Nano Energy, 2022, 98, 107281.	8.2	11
13	Silver Nanowire Composite Electrode Enabling Highly Flexible, Robust Organic Photovoltaics. Solar Rrl, 2022, 6, .	3.1	6
14	A Topâ€Down Strategy to Engineer ActiveLayer Morphology for Highly Efficient and Stable Allâ€Polymer Solar Cells. Advanced Materials, 2022, 34, .	11.1	41
15	Achieving 19% Power Conversion Efficiency in Planarâ€Mixed Heterojunction Organic Solar Cells Using a Pseudosymmetric Electron Acceptor. Advanced Materials, 2022, 34, .	11.1	271
16	Revealing aggregation of non-fullerene acceptors in intermixed phase by ultraviolet-visible absorption spectroscopy. Cell Reports Physical Science, 2022, 3, 100983.	2.8	6
17	Optimized Active Layer Morphologies via Ternary Copolymerization of Polymer Donors for 17.6 % Efficiency Organic Solar Cells with Enhanced Fill Factor. Angewandte Chemie, 2021, 133, 2352-2359.	1.6	21
18	Optimized Active Layer Morphologies via Ternary Copolymerization of Polymer Donors for 17.6 % Efficiency Organic Solar Cells with Enhanced Fill Factor. Angewandte Chemie - International Edition, 2021, 60, 2322-2329.	7.2	138

#	Article	IF	CITATIONS
19	Asymmetric Alkoxy and Alkyl Substitution on Nonfullerene Acceptors Enabling Highâ€Performance Organic Solar Cells. Advanced Energy Materials, 2021, 11, 2003141.	10.2	144
20	Carboxylate substituted pyrazine: A simple and low-cost building block for novel wide bandgap polymer donor enables 15.3% efficiency in organic solar cells. Nano Energy, 2021, 82, 105679.	8.2	48
21	Silicon Phthalocyanines for n-Type Organic Thin-Film Transistors: Development of Structure–Property Relationships. ACS Applied Electronic Materials, 2021, 3, 325-336.	2.0	27
22	Functionalization of Benzotriazole-Based Conjugated Polymers for Solar Cells: Heteroatom vs Substituents. ACS Applied Polymer Materials, 2021, 3, 30-41.	2.0	14
23	High performance tandem organic solar cells via a strongly infrared-absorbing narrow bandgap acceptor. Nature Communications, 2021, 12, 178.	5.8	122
24	A History and Perspective of Nonâ€Fullerene Electron Acceptors for Organic Solar Cells. Advanced Energy Materials, 2021, 11, 2003570.	10.2	323
25	Optically Probing Field-Dependent Charge Dynamics in Non-Fullerene Organic Photovoltaics with Small Interfacial Energy Offsets. Journal of Physical Chemistry C, 2021, 125, 1714-1722.	1.5	5
26	Modulation of Morphological, Mechanical, and Photovoltaic Properties of Ternary Organic Photovoltaic Blends for Optimum Operation. Advanced Energy Materials, 2021, 11, 2003506.	10.2	92
27	Pseudo-bilayer architecture enables high-performance organic solar cells with enhanced exciton diffusion length. Nature Communications, 2021, 12, 468.	5.8	137
28	A molecular interaction–diffusion framework for predicting organic solar cell stability. Nature Materials, 2021, 20, 525-532.	13.3	212
29	Relationship between charge transfer state electroluminescence and the degradation of organic photovoltaics. Applied Physics Letters, 2021, 118, .	1.5	4
30	Reducing Energy Disorder of Hole Transport Layer by Charge Transfer Complex for High Performance p–i–n Perovskite Solar Cells. Advanced Materials, 2021, 33, e2006753.	11.1	69
31	Effect of Palladiumâ€Tetrakis(Triphenylphosphine) Catalyst Traces on Charge Recombination and Extraction in Nonâ€Fullereneâ€based Organic Solar Cells. Advanced Functional Materials, 2021, 31, 2009363.	7.8	27
32	Balancing crop production and energy harvesting in organic solar-powered greenhouses. Cell Reports Physical Science, 2021, 2, 100381.	2.8	48
33	Regioâ€Regular Polymer Acceptors Enabled by Determined Fluorination on End Groups for Allâ€Polymer Solar Cells with 15.2 % Efficiency. Angewandte Chemie, 2021, 133, 10225-10234.	1.6	13
34	Regioâ€Regular Polymer Acceptors Enabled by Determined Fluorination on End Groups for Allâ€Polymer Solar Cells with 15.2 % Efficiency. Angewandte Chemie - International Edition, 2021, 60, 10137-10146.	7.2	145
35	Orientational Ordering within Semiconducting Polymer Fibrils. Advanced Functional Materials, 2021, 31, 2102522.	7.8	3
36	A Difluoroâ€Monobromo End Group Enables Highâ€Performance Polymer Acceptor and Efficient Allâ€Polymer Solar Cells Processable with Green Solvent under Ambient Condition. Advanced Functional Materials, 2021, 31, 2100791.	7.8	89

#	Article	IF	CITATIONS
37	A Chlorinated Donor Polymer Achieving Highâ€Performance Organic Solar Cells with a Wide Range of Polymer Molecular Weight. Advanced Functional Materials, 2021, 31, 2102413.	7.8	69
38	Insights into Bulkâ€Heterojunction Organic Solar Cells Processed from Green Solvent. Solar Rrl, 2021, 5, 2100213.	3.1	30
39	Designing Simple Conjugated Polymers for Scalable and Efficient Organic Solar Cells. ChemSusChem, 2021, 14, 3561-3568.	3.6	36
40	Timescales of excited state relaxation in <mml:math xmlns:mml="http://www.w3.org/1998/Math/MathML"><mml:mrow><mml:mi>α</mml:mi><mml:mtext>â^'observed by time-resolved two-photon photoemission spectroscopy. Physical Review B, 2021, 103, .</mml:mtext></mml:mrow></mml:math 	nl:mutext><	m r nl:mi>Ru<
41	The performance-stability conundrum of BTP-based organic solar cells. Joule, 2021, 5, 2129-2147.	11.7	133
42	Polymerized small molecular acceptor based all-polymer solar cells with an efficiency of 16.16% via tuning polymer blend morphology by molecular design. Nature Communications, 2021, 12, 5264.	5.8	170
43	Non-fullerene acceptor organic photovoltaics with intrinsic operational lifetimes over 30 years. Nature Communications, 2021, 12, 5419.	5.8	128
44	Optimization of active layer morphology by small-molecule donor design enables over 15% efficiency in small-molecule organic solar cells. Journal of Materials Chemistry A, 2021, 9, 13653-13660.	5.2	21
45	Baseplate Temperatureâ€Dependent Vertical Composition Gradient in Pseudoâ€Bilayer Films for Printing Nonâ€Fullerene Organic Solar Cells. Advanced Energy Materials, 2021, 11, 2102135.	10.2	33
46	Alkyl hain Branching of Nonâ€Fullerene Acceptors Flanking Conjugated Side Groups toward Highly Efficient Organic Solar Cells. Advanced Energy Materials, 2021, 11, 2102596.	10.2	125
47	Upper and Apparent Lower Critical Solution Temperature Branches in the Phase Diagram of Polymer:Small Molecule Semiconducting Systems. Journal of Physical Chemistry Letters, 2021, 12, 10845-10853.	2.1	7
48	Effects of Shortâ€Axis Alkoxy Substituents on Molecular Selfâ€Assembly and Photovoltaic Performance of Indacenodithiopheneâ€Based Acceptors. Advanced Functional Materials, 2020, 30, 1906855.	7.8	50
49	Side-chain engineering of medium bandgap polymer donors for efficient polymer solar cells. Organic Electronics, 2020, 78, 105603.	1.4	5
50	Millimeter wave direct-current transmission and reflection spectral data of some organic photo-responsive materials. Data in Brief, 2020, 28, 104996.	0.5	0
51	Balanced Charge Transport Optimizes Industryâ€Relevant Ternary Polymer Solar Cells. Solar Rrl, 2020, 4, 2000538.	3.1	15
52	Impact of Isomer Design on Physicochemical Properties and Performance in High-Efficiency All-Polymer Solar Cells. Macromolecules, 2020, 53, 9026-9033.	2.2	25
53	Enhanced efficiency in nonfullerene organic solar cells by tuning molecular order and domain characteristics. Nano Energy, 2020, 77, 105310.	8.2	25
54	Investigating the active layer thickness dependence of non-fullerene organic solar cells based on PM7 derivatives. Journal of Materials Chemistry C, 2020, 8, 15459-15469.	2.7	16

#	Article	IF	CITATIONS
55	Organic Solar Cells with Large Insensitivity to Donor Polymer Molar Mass across All Acceptor Classes. ACS Applied Polymer Materials, 2020, 2, 5300-5308.	2.0	7
56	Incorporation of alkylthio side chains on benzothiadiazole-based non-fullerene acceptors enables high-performance organic solar cells with over 16% efficiency. Journal of Materials Chemistry A, 2020, 8, 23239-23247.	5.2	39
57	Deciphering the Role of Chalcogen-Containing Heterocycles in Nonfullerene Acceptors for Organic Solar Cells. ACS Energy Letters, 2020, 5, 3415-3425.	8.8	73
58	Long-range exciton diffusion in molecular non-fullerene acceptors. Nature Communications, 2020, 11, 5220.	5.8	204
59	Effect of the chlorine substitution position of the end-group on intermolecular interactions and photovoltaic performance of small molecule acceptors. Energy and Environmental Science, 2020, 13, 5028-5038.	15.6	56
60	Tailoring non-fullerene acceptors using selenium-incorporated heterocycles for organic solar cells with over 16% efficiency. Journal of Materials Chemistry A, 2020, 8, 23756-23765.	5.2	85
61	Selective Hole and Electron Transport in Efficient Quaternary Blend Organic Solar Cells. Joule, 2020, 4, 1790-1805.	11.7	110
62	Random Polymerization Strategy Leads to a Family of Donor Polymers Enabling Wellâ€Controlled Morphology and Multiple Cases of Highâ€Performance Organic Solar Cells. Advanced Materials, 2020, 32, e2003500.	11.1	59
63	Enhanced mid-wavelength infrared refractive index of organically modified chalcogenide (ORMOCHALC) polymer nanocomposites with thermomechanical stability. Optical Materials, 2020, 108, 110197.	1.7	12
64	Novel Bimodal Silver Nanowire Network as Top Electrodes for Reproducible and Highâ€Efficiency Semitransparent Organic Photovoltaics. Solar Rrl, 2020, 4, 2000328.	3.1	36
65	Precise Control of Phase Separation Enables 12% Efficiency in All Small Molecule Solar Cells. Advanced Energy Materials, 2020, 10, 2001589.	10.2	33
66	Efficient Organic Ternary Solar Cells Employing Narrow Band Gap Diketopyrrolopyrrole Polymers and Nonfullerene Acceptors. Chemistry of Materials, 2020, 32, 7309-7317.	3.2	22
67	Color-neutral, semitransparent organic photovoltaics for power window applications. Proceedings of the United States of America, 2020, 117, 21147-21154.	3.3	109
68	The role of bulk and interfacial morphology in charge generation, recombination, and extraction in non-fullerene acceptor organic solar cells. Energy and Environmental Science, 2020, 13, 3679-3692.	15.6	126
69	Effect of main and side chain chlorination on the photovoltaic properties of benzodithiophene- <i>alt</i> -benzotriazole polymers. Journal of Materials Chemistry C, 2020, 8, 15426-15435.	2.7	10
70	Modulating Energy Level on an Aâ€Dâ€A′â€Dâ€Aâ€Type Unfused Acceptor by a Benzothiadiazole Core Enable Organic Solar Cells with Simple Procedure and High Performance. Solar RrI, 2020, 4, 2000421.	^{2S} 3.1	48
71	Low Temperature Aggregation Transitions in N3 and Y6 Acceptors Enable Doubleâ€Annealing Method That Yields Hierarchical Morphology and Superior Efficiency in Nonfullerene Organic Solar Cells. Advanced Functional Materials, 2020, 30, 2005011.	7.8	66
72	Morphological–Electrical Property Relation in Cu(In,Ga)(S,Se) ₂ Solar Cells: Significance of Crystal Grain Growth and Band Grading by Potassium Treatment. Small, 2020, 16, e2003865.	5.2	12

Harald Ade

#	Article	IF	CITATIONS
73	The Role of Demixing and Crystallization Kinetics on the Stability of Nonâ€Fullerene Organic Solar Cells. Advanced Materials, 2020, 32, e2005348.	11.1	74
74	Thermodynamic Properties and Molecular Packing Explain Performance and Processing Procedures of Three D18:NFA Organic Solar Cells. Advanced Materials, 2020, 32, e2005386.	11.1	130
75	The Critical Role of Materials' Interaction in Realizing Organic Field-Effect Transistors Via High-Dilution Blending with Insulating Polymers. ACS Applied Materials & Interfaces, 2020, 12, 26239-26249.	4.0	22
76	Highâ€Performance Allâ€Polymer Solar Cells: Synthesis of Polymer Acceptor by a Random Ternary Copolymerization Strategy. Angewandte Chemie - International Edition, 2020, 59, 15181-15185.	7.2	136
77	Highâ€Performance Allâ€Polymer Solar Cells: Synthesis of Polymer Acceptor by a Random Ternary Copolymerization Strategy. Angewandte Chemie, 2020, 132, 15293-15297.	1.6	18
78	Highâ€Performance Tandem Organic Solar Cells Using HSolar as the Interconnecting Layer. Advanced Energy Materials, 2020, 10, 2000823.	10.2	23
79	Optimization Requirements of Efficient Polythiophene:Nonfullerene Organic Solar Cells. Joule, 2020, 4, 1278-1295.	11.7	133
80	Synergistic Use of Pyridine and Selenophene in a Diketopyrrolopyrroleâ€Based Conjugated Polymer Enhances the Electron Mobility in Organic Transistors. Advanced Functional Materials, 2020, 30, 2000489.	7.8	43
81	Unifying Charge Generation, Recombination, and Extraction in Lowâ€Offset Nonâ€Fullerene Acceptor Organic Solar Cells. Advanced Energy Materials, 2020, 10, 2001203.	10.2	74
82	Enhanced hindrance from phenyl outer side chains on nonfullerene acceptor enables unprecedented simultaneous enhancement in organic solar cell performances with 16.7% efficiency. Nano Energy, 2020, 76, 105087.	8.2	85
83	Role of Secondary Thermal Relaxations in Conjugated Polymer Film Toughness. Chemistry of Materials, 2020, 32, 6540-6549.	3.2	27
84	Organic Solar Cells: Highâ€₽erformance Tandem Organic Solar Cells Using HSolar as the Interconnecting Layer (Adv. Energy Mater. 25/2020). Advanced Energy Materials, 2020, 10, 2070109.	10.2	0
85	3,4â€Dicyanothiophene—a Versatile Building Block for Efficient Nonfullerene Polymer Solar Cells. Advanced Energy Materials, 2020, 10, 1904247.	10.2	48
86	Achieving Net Zero Energy Greenhouses by Integrating Semitransparent Organic Solar Cells. Joule, 2020, 4, 490-506.	11.7	179
87	Efficient Energy Funneling in Quasiâ€2D Perovskites: From Light Emission to Lasing. Advanced Materials, 2020, 32, e1906571.	11.1	134
88	Near-infrared electron acceptors with fused nonacyclic molecular backbones for nonfullerene organic solar cells. Materials Chemistry Frontiers, 2020, 4, 1729-1738.	3.2	23
89	Critical Role of Polymer Aggregation and Miscibility in Nonfullereneâ€Based Organic Photovoltaics. Advanced Energy Materials, 2020, 10, 1902430.	10.2	41
90	Asymmetrically noncovalently fused-ring acceptor for high-efficiency organic solar cells with reduced voltage loss and excellent thermal stability. Nano Energy, 2020, 74, 104861.	8.2	75

Harald Ade

#	Article	IF	CITATIONS
91	Green solvent-processed organic solar cells based on a low cost polymer donor and a small molecule acceptor. Journal of Materials Chemistry C, 2020, 8, 7718-7724.	2.7	40
92	A 3D nonfullerene electron acceptor with a 9,9′-bicarbazole backbone for high-efficiency organic solar cells. Organic Electronics, 2020, 84, 105784.	1.4	5
93	Reduced Nonradiative Energy Loss Caused by Aggregation of Nonfullerene Acceptor in Organic Solar Cells. Advanced Energy Materials, 2019, 9, 1901823.	10.2	72
94	A multi-objective optimization-based layer-by-layer blade-coating approach for organic solar cells: rational control of vertical stratification for high performance. Energy and Environmental Science, 2019, 12, 3118-3132.	15.6	142
95	Utilizing Difluorinated Thiophene Units To Improve the Performance of Polymer Solar Cells. Macromolecules, 2019, 52, 6523-6532.	2.2	14
96	The Importance of Entanglements in Optimizing the Mechanical and Electrical Performance of All-Polymer Solar Cells. Chemistry of Materials, 2019, 31, 5124-5132.	3.2	88
97	High voltage all polymer solar cells with a polymer acceptor based on NDI and benzotriazole. Journal of Materials Chemistry C, 2019, 7, 9031-9037.	2.7	7
98	Alkyl Chain Tuning of Small Molecule Acceptors for Efficient Organic Solar Cells. Joule, 2019, 3, 3020-3033.	11.7	763
99	Modulation of Building Block Size in Conjugated Polymers with D–A Structure for Polymer Solar Cells. Macromolecules, 2019, 52, 7929-7938.	2.2	10
100	Effect of Cyano Substitution on Conjugated Polymers for Bulk Heterojunction Solar Cells. ACS Applied Polymer Materials, 2019, 1, 3313-3322.	2.0	17
101	Conjugationâ€Curtailing of Benzodithionopyranâ€Cored Molecular Acceptor Enables Efficient Airâ€Processed Small Molecule Solar Cells. Small, 2019, 15, e1902656.	5.2	11
102	Multi-length scale morphology of nonfullerene all-small molecule blends and its relation to device function in organic solar cells. Materials Chemistry Frontiers, 2019, 3, 137-144.	3.2	12
103	A decacyclic indacenodithiophene-based non-fullerene electron acceptor with meta-alkyl-phenyl substitutions for polymer solar cells. Journal of Materials Chemistry A, 2019, 7, 4063-4071.	5.2	17
104	Enhanced JSC of P3HT-based non-fullerene polymer solar cells by modulating aggregation effect of P3HT in solution state. Organic Electronics, 2019, 68, 15-21.	1.4	17
105	Black phosphorus nanoflakes as morphology modifier for efficient fullerene-free organic solar cells with high fill-factor and better morphological stability. Nano Research, 2019, 12, 777-783.	5.8	31
106	Chlorinated Thiophene End Groups for Highly Crystalline Alkylated Non-Fullerene Acceptors toward Efficient Organic Solar Cells. Chemistry of Materials, 2019, 31, 6672-6676.	3.2	48
107	Efficient DPP Donor and Nonfullerene Acceptor Organic Solar Cells with High Photonâ€ŧo urrent Ratio and Low Energetic Loss. Advanced Functional Materials, 2019, 29, 1902441.	7.8	43
108	Effect of Replacing Thiophene by Selenophene on the Photovoltaic Performance of Wide Bandgap Copolymer Donors. Macromolecules, 2019, 52, 4776-4784.	2.2	26

#	Article	IF	CITATIONS
109	Temperatureâ€Dependent Aggregation Donor Polymers Enable Highly Efficient Sequentially Processed Organic Photovoltaics Without the Need of Orthogonal Solvents. Advanced Functional Materials, 2019, 29, 1902478.	7.8	50
110	Quantifying and Understanding Voltage Losses Due to Nonradiative Recombination in Bulk Heterojunction Organic Solar Cells with Low Energetic Offsets. Advanced Energy Materials, 2019, 9, 1901077.	10.2	69
111	Aryl-Perfluoroaryl Interaction in Two-Dimensional Organic–Inorganic Hybrid Perovskites Boosts Stability and Photovoltaic Efficiency. , 2019, 1, 171-176.		63
112	The crucial role of end group planarity for fused-ring electron acceptors in organic solar cells. Materials Chemistry Frontiers, 2019, 3, 1642-1652.	3.2	12
113	Delineation of Thermodynamic and Kinetic Factors that Control Stability in Non-fullerene Organic Solar Cells. Joule, 2019, 3, 1328-1348.	11.7	143
114	Intramolecular ï€-stacked perylene-diimide acceptors for non-fullerene organic solar cells. Journal of Materials Chemistry A, 2019, 7, 8136-8143.	5.2	34
115	Synthetic control over orientational degeneracy of spacer cations enhances solar cell efficiency in two-dimensional perovskites. Nature Communications, 2019, 10, 1276.	5.8	222
116	The impact of fluorination on both donor polymer and non-fullerene acceptor: The more fluorine, the merrier. Nano Research, 2019, 12, 2400-2405.	5.8	28
117	Sequential Deposition of Organic Films with Ecoâ€Compatible Solvents Improves Performance and Enables Over 12%â€Efficiency Nonfullerene Solar Cells. Advanced Materials, 2019, 31, e1808153.	11.1	132
118	Highly Efficient, Stable, and Ductile Ternary Nonfullerene Organic Solar Cells from a Twoâ€Donor Polymer Blend. Advanced Materials, 2019, 31, e1808279.	11.1	79
119	Rational Strategy to Stabilize an Unstable Highâ€Efficiency Binary Nonfullerene Organic Solar Cells with a Third Component. Advanced Energy Materials, 2019, 9, 1900376.	10.2	132
120	Dual Sensitizer and Processing-Aid Behavior of Donor Enables Efficient Ternary Organic Solar Cells. Joule, 2019, 3, 846-857.	11.7	84
121	Efficient Thick-Film Polymer Solar Cells with Enhanced Fill Factors via Increased Fullerene Loading. ACS Applied Materials & Interfaces, 2019, 11, 10794-10800.	4.0	21
122	Polymer Side-Chain Variation Induces Microstructural Disparity in Nonfullerene Solar Cells. Chemistry of Materials, 2019, 31, 6568-6577.	3.2	45
123	Unveiling the operation mechanism of layered perovskite solar cells. Nature Communications, 2019, 10, 1008.	5.8	216
124	"Twisted―conjugated molecules as donor materials for efficient all-small-molecule organic solar cells processed with tetrahydrofuran. Journal of Materials Chemistry A, 2019, 7, 23008-23018.	5.2	37
125	The Critical Impact of Material and Process Compatibility on the Active Layer Morphology and Performance of Organic Ternary Solar Cells. Advanced Energy Materials, 2019, 9, 1802293.	10.2	35
126	Revealing the Impact of F4â€TCNQ as Additive on Morphology and Performance of Highâ€Efficiency Nonfullerene Organic Solar Cells. Advanced Functional Materials, 2019, 29, 1806262.	7.8	55

#	Article	IF	CITATIONS
127	A Printable Organic Cathode Interlayer Enables over 13% Efficiency for 1-cm2 Organic Solar Cells. Joule, 2019, 3, 227-239.	11.7	193
128	Efficient All-Polymer Solar Cells based on a New Polymer Acceptor Achieving 10.3% Power Conversion Efficiency. ACS Energy Letters, 2019, 4, 417-422.	8.8	196
129	Competition between Exceptionally Longâ€Range Alkyl Sidechain Ordering and Backbone Ordering in Semiconducting Polymers and Its Impact on Electronic and Optoelectronic Properties. Advanced Functional Materials, 2019, 29, 1806977.	7.8	31
130	Quenching to the Percolation Threshold in Organic Solar Cells. Joule, 2019, 3, 443-458.	11.7	183
131	Isomeryâ€Dependent Miscibility Enables Highâ€Performance Allâ€Smallâ€Molecule Solar Cells. Small, 2019, 15, 1804271.	5.2	50
132	Rigid valence band shift due to molecular surface counter-doping of MoS2. Surface Science, 2019, 679, 254-258.	0.8	9
133	Soft X-Ray Scattering Characterization of Polymer Semiconductors. , 2019, , 427-458.		9
134	Solar Cells: Surpassing 10% Efficiency Benchmark for Nonfullerene Organic Solar Cells by Scalable Coating in Air from Single Nonhalogenated Solvent (Adv. Mater. 8/2018). Advanced Materials, 2018, 30, 1870054.	11.1	3
135	The Role of FRET in Non-Fullerene Organic Solar Cells: Implications for Molecular Design. Journal of Physical Chemistry A, 2018, 122, 3764-3771.	1.1	18
136	Molecular engineering of perylene-diimide-based polymer acceptors containing heteroacene units for all-polymer solar cells. Organic Electronics, 2018, 58, 222-230.	1.4	15
137	Quantitative relations between interaction parameter, miscibility and function in organic solar cells. Nature Materials, 2018, 17, 253-260.	13.3	556
138	Miscibility–Function Relations in Organic Solar Cells: Significance of Optimal Miscibility in Relation to Percolation. Advanced Energy Materials, 2018, 8, 1703058.	10.2	223
139	Integrated circuits based on conjugated polymer monolayer. Nature Communications, 2018, 9, 451.	5.8	69
140	A polymer design strategy toward green solvent processed efficient non-fullerene polymer solar cells. Journal of Materials Chemistry A, 2018, 6, 4324-4330.	5.2	48
141	Controlling Blend Morphology for Ultrahigh Current Density in Nonfullerene Acceptor-Based Organic Solar Cells. ACS Energy Letters, 2018, 3, 669-676.	8.8	242
142	Multiple Cases of Efficient Nonfullerene Ternary Organic Solar Cells Enabled by an Effective Morphology Control Method. Advanced Energy Materials, 2018, 8, 1701370.	10.2	140
143	Alkyl Chain Regiochemistry of Benzotriazoleâ€Based Donor Polymers Influencing Morphology and Performances of Nonâ€Fullerene Organic Solar Cells. Advanced Energy Materials, 2018, 8, 1702427.	10.2	36
144	Surpassing 10% Efficiency Benchmark for Nonfullerene Organic Solar Cells by Scalable Coating in Air from Single Nonhalogenated Solvent. Advanced Materials, 2018, 30, 1705485.	11.1	150

#	Article	IF	CITATIONS
145	A Highâ€Efficiency Organic Solar Cell Enabled by the Strong Intramolecular Electron Push–Pull Effect of the Nonfullerene Acceptor. Advanced Materials, 2018, 30, e1707170.	11.1	351
146	Influence of Donor Polymer on the Molecular Ordering of Small Molecular Acceptors in Nonfullerene Polymer Solar Cells. Advanced Energy Materials, 2018, 8, 1701674.	10.2	60
147	Highâ€Performance Wide Bandgap Copolymers Using an EDOT Modified Benzodithiophene Donor Block with 10.11% Efficiency. Advanced Energy Materials, 2018, 8, 1602773.	10.2	35
148	A Facile Method to Fineâ€Tune Polymer Aggregation Properties and Blend Morphology of Polymer Solar Cells Using Donor Polymers with Randomly Distributed Alkyl Chains. Advanced Energy Materials, 2018, 8, 1701895.	10.2	62
149	Charge Generation and Recombination in an Organic Solar Cell with Low Energetic Offsets. Advanced Energy Materials, 2018, 8, 1701073.	10.2	60
150	Effect of Alkylsilyl Sideâ€Chain Structure on Photovoltaic Properties of Conjugated Polymer Donors. Advanced Energy Materials, 2018, 8, 1702324.	10.2	102
151	Soft X-ray Microscopy: History, Status, and Future. Microscopy and Microanalysis, 2018, 24, 1000-1001.	0.2	0
152	Impact of Nonfullerene Molecular Architecture on Charge Generation, Transport, and Morphology in PTB7â€Thâ€Based Organic Solar Cells. Advanced Functional Materials, 2018, 28, 1802702.	7.8	44
153	Donor polymer based on alkylthiophene side chains for efficient non-fullerene organic solar cells: insights into fluorination and side chain effects on polymer aggregation and blend morphology. Journal of Materials Chemistry A, 2018, 6, 23270-23277.	5.2	16
154	A time-resolved millimeter wave conductivity (TR-mmWC) apparatus for charge dynamical properties of semiconductors. Review of Scientific Instruments, 2018, 89, 104704.	0.6	7
155	The finale of a trilogy: comparing terpolymers and ternary blends with structurally similar backbones for use in organic bulk heterojunction solar cells. Journal of Materials Chemistry A, 2018, 6, 19190-19200.	5.2	13
156	Measuring Temperature-Dependent Miscibility for Polymer Solar Cell Blends: An Easily Accessible Optical Method Reveals Complex Behavior. Chemistry of Materials, 2018, 30, 3943-3951.	3.2	38
157	Highâ€Efficiency Allâ€Smallâ€Molecule Organic Solar Cells Based on an Organic Molecule Donor with Alkylsilylâ€Thienyl Conjugated Side Chains. Advanced Materials, 2018, 30, e1706361.	11.1	154
158	Effect of Side-Chain Engineering of Bithienylbenzodithiophene- <i>alt</i> -fluorobenzotriazole-Based Copolymers on the Thermal Stability and Photovoltaic Performance of Polymer Solar Cells. Macromolecules, 2018, 51, 6028-6036.	2.2	47
159	Effect of Ringâ€Fusion on Miscibility and Domain Purity: Key Factors Determining the Performance of PDIâ€Based Nonfullerene Organic Solar Cells. Advanced Energy Materials, 2018, 8, 1800234.	10.2	75
160	Modulation of End Groups for Lowâ€Bandgap Nonfullerene Acceptors Enabling Highâ€Performance Organic Solar Cells. Advanced Energy Materials, 2018, 8, 1801203.	10.2	99
161	Effects of fused-ring regiochemistry on the properties and photovoltaic performance of n-type organic semiconductor acceptors. Journal of Materials Chemistry A, 2018, 6, 15933-15941.	5.2	25
162	A Highly Crystalline Fusedâ€Ring nâ€Type Small Molecule for Nonâ€Fullerene Acceptor Based Organic Solar Cells and Fieldâ€Effect Transistors. Advanced Functional Materials, 2018, 28, 1802895.	7.8	74

#	Article	IF	CITATIONS
163	Long-Lived, Non-Geminate, Radiative Recombination of Photogenerated Charges in a Polymer/Small-Molecule Acceptor Photovoltaic Blend. Journal of the American Chemical Society, 2018, 140, 9996-10008.	6.6	73
164	A Wide Band Gap Polymer with a Deep Highest Occupied Molecular Orbital Level Enables 14.2% Efficiency in Polymer Solar Cells. Journal of the American Chemical Society, 2018, 140, 7159-7167.	6.6	654
165	Shear-Enhanced Transfer Printing of Conducting Polymer Thin Films. ACS Applied Materials & Interfaces, 2018, 10, 31560-31567.	4.0	34
166	Carboxylate substitution position influencing polymer properties and enabling non-fullerene organic solar cells with high open circuit voltage and low voltage loss. Journal of Materials Chemistry A, 2018, 6, 16874-16881.	5.2	15
167	Polymer non-fullerene solar cells of vastly different efficiencies for minor side-chain modification: impact of charge transfer, carrier lifetime, morphology and mobility. Journal of Materials Chemistry A, 2018, 6, 12484-12492.	5.2	43
168	Improvement of Photovoltaic Performance of Polymer Solar Cells by Rational Molecular Optimization of Organic Molecule Acceptors. Advanced Energy Materials, 2018, 8, 1800815.	10.2	36
169	Competition between exceptionally long-range alkyl sidechain ordering and backbone ordering in semiconducting polymers and its impact on electronic and optoelectronic properties. Advanced Functional Materials, 2018, 29, .	7.8	0
170	Comparing non-fullerene acceptors with fullerene in polymer solar cells: a case study with FTAZ and PyCNTAZ. Journal of Materials Chemistry A, 2017, 5, 4886-4893.	5.2	44
171	Surprising Effects upon Inserting Benzene Units into a Quaterthiopheneâ€Based Dâ€A Polymer–Improving Nonâ€Fullerene Organic Solar Cells via Donor Polymer Design. Advanced Energy Materials, 2017, 7, 1602304.	10.2	57
172	Side-chain engineering of perylenediimide-vinylene polymer acceptors for high-performance all-polymer solar cells. Materials Chemistry Frontiers, 2017, 1, 1362-1368.	3.2	24
173	Efficient Nonfullerene Polymer Solar Cells Enabled by a Novel Wide Bandgap Small Molecular Acceptor. Advanced Materials, 2017, 29, 1606054.	11.1	181
174	Flexible Inorganic Ferroelectric Thin Films for Nonvolatile Memory Devices. Advanced Functional Materials, 2017, 27, 1700461.	7.8	111
175	Morphological characterization of fullerene and fullerene-free organic photovoltaics by combined real and reciprocal space techniques. Journal of Materials Research, 2017, 32, 1921-1934.	1.2	28
176	Significant Influence of the Methoxyl Substitution Position on Optoelectronic Properties and Molecular Packing of Smallâ€Molecule Electron Acceptors for Photovoltaic Cells. Advanced Energy Materials, 2017, 7, 1700183.	10.2	184
177	Improved Performance of Allâ€Polymer Solar Cells Enabled by Naphthodiperylenetetraimideâ€Based Polymer Acceptor. Advanced Materials, 2017, 29, 1700309.	11.1	306
178	Quantitative Morphology–Performance Correlations in Organic Solar Cells: Insights from Soft Xâ€Ray Scattering. Advanced Energy Materials, 2017, 7, 1700084.	10.2	123
179	A regioregular conjugated polymer for high performance thick-film organic solar cells without processing additive. Journal of Materials Chemistry A, 2017, 5, 10517-10525.	5.2	46
180	Charge Generation and Mobility-Limited Performance of Bulk Heterojunction Solar Cells with a Higher Adduct Fullerene. Journal of Physical Chemistry C, 2017, 121, 10305-10316.	1.5	11

#	Article	IF	CITATIONS
181	Panchromatic Sequentially Cast Ternary Polymer Solar Cells. Advanced Materials, 2017, 29, 1604603.	11.1	87
182	Strong polymer molecular weight-dependent material interactions: impact on the formation of the polymer/fullerene bulk heterojunction morphology. Journal of Materials Chemistry A, 2017, 5, 13176-13188.	5.2	49
183	Morphology control enables thickness-insensitive efficient nonfullerene polymer solar cells. Materials Chemistry Frontiers, 2017, 1, 2057-2064.	3.2	42
184	Achieving Highly Efficient Nonfullerene Organic Solar Cells with Improved Intermolecular Interaction and Open ircuit Voltage. Advanced Materials, 2017, 29, 1700254.	11.1	363
185	Crystallization of Sensitizers Controls Morphology and Performance in Si-/C-PCPDTBT-Sensitized P3HT:ICBA Ternary Blends. Macromolecules, 2017, 50, 2415-2423.	2.2	27
186	9.73% Efficiency Nonfullerene All Organic Small Molecule Solar Cells with Absorption-Complementary Donor and Acceptor. Journal of the American Chemical Society, 2017, 139, 5085-5094.	6.6	303
187	Highâ€Efficiency Nonfullerene Organic Solar Cells: Critical Factors that Affect Complex Multiâ€Length Scale Morphology and Device Performance. Advanced Energy Materials, 2017, 7, 1602000.	10.2	232
188	A random donor polymer based on an asymmetric building block to tune the morphology of non-fullerene organic solar cells. Journal of Materials Chemistry A, 2017, 5, 22480-22488.	5.2	12
189	Donor polymer fluorination doubles the efficiency in non-fullerene organic photovoltaics. Journal of Materials Chemistry A, 2017, 5, 22536-22541.	5.2	27
190	Importance of 2D Conjugated Side Chains of Benzodithiophene-Based Polymers in Controlling Polymer Packing, Interfacial Ordering, and Composition Variations of All-Polymer Solar Cells. Chemistry of Materials, 2017, 29, 9407-9415.	3.2	67
191	Design of a New Smallâ€Molecule Electron Acceptor Enables Efficient Polymer Solar Cells with High Fill Factor. Advanced Materials, 2017, 29, 1704051.	11.1	224
192	Connecting Molecular Conformation to Aggregation in P3HT Using Near Edge X-ray Absorption Fine Structure Spectroscopy. Journal of Physical Chemistry C, 2017, 121, 21720-21728.	1.5	19
193	Monitoring Charge Separation Processes in Quasi-One-Dimensional Organic Crystalline Structures. Nano Letters, 2017, 17, 6056-6061.	4.5	5
194	Precise Manipulation of Multilength Scale Morphology and Its Influence on Ecoâ€Friendly Printed Allâ€Polymer Solar Cells. Advanced Functional Materials, 2017, 27, 1702016.	7.8	99
195	Gaining further insight into the effects of thermal annealing and solvent vapor annealing on time morphological development and degradation in small molecule solar cells. Journal of Materials Chemistry A, 2017, 5, 18101-18110.	5.2	50
196	Environmentally-friendly solvent processed fullerene-free organic solar cells enabled by screening halogen-free solvent additives. Science China Materials, 2017, 60, 697-706.	3.5	33
197	Role of Polymer Segregation on the Mechanical Behavior of All-Polymer Solar Cell Active Layers. ACS Applied Materials & Interfaces, 2017, 9, 43886-43892.	4.0	40
198	Synthesis of High-Crystallinity DPP Polymers with Balanced Electron and Hole Mobility. Chemistry of Materials, 2017, 29, 10220-10232.	3.2	40

#	Article	IF	CITATIONS
199	Ring-Fusion of Perylene Diimide Acceptor Enabling Efficient Nonfullerene Organic Solar Cells with a Small Voltage Loss. Journal of the American Chemical Society, 2017, 139, 16092-16095.	6.6	304
200	Synthesis and Photovoltaic Properties of a Series of Narrow Bandgap Organic Semiconductor Acceptors with Their Absorption Edge Reaching 900 nm. Chemistry of Materials, 2017, 29, 10130-10138.	3.2	93
201	Fluorinated Thiophene Units Improve Photovoltaic Device Performance of Donor–Acceptor Copolymers. Chemistry of Materials, 2017, 29, 5990-6002.	3.2	57
202	Control of Mesoscale Morphology and Photovoltaic Performance in Diketopyrrolopyrroleâ€Based Small Band Gap Terpolymers. Advanced Energy Materials, 2017, 7, 1601138.	10.2	59
203	Efficient Charge Transfer and Fineâ€Tuned Energy Level Alignment in a THFâ€Processed Fullereneâ€Free Organic Solar Cell with 11.3% Efficiency. Advanced Materials, 2017, 29, 1604241.	11.1	305
204	Charge Creation and Recombination in Multi‣ength Scale Polymer:Fullerene BHJ Solar Cell Morphologies. Advanced Energy Materials, 2016, 6, 1600699.	10.2	85
205	Lowest energy Frenkel and charge transfer exciton intermixing in one-dimensional copper phthalocyanine molecular lattice. Applied Physics Letters, 2016, 109, 213302.	1.5	16
206	Charge Photogeneration in Organic Photovoltaics: Role of Hot versus Cold Chargeâ€Transfer Excitons. Advanced Energy Materials, 2016, 6, 1301032.	10.2	16
207	Organic Photovoltaics: Charge Photogeneration in Organic Photovoltaics: Role of Hot versus Cold Chargeâ€Iransfer Excitons (Adv. Energy Mater. 1/2016). Advanced Energy Materials, 2016, 6, .	10.2	1
208	Energyâ€Level Modulation of Smallâ€Molecule Electron Acceptors to Achieve over 12% Efficiency in Polymer Solar Cells. Advanced Materials, 2016, 28, 9423-9429.	11.1	1,307
209	High Performance Organic Solar Cells Processed by Blade Coating in Air from a Benign Food Additive Solution. Chemistry of Materials, 2016, 28, 7451-7458.	3.2	91
210	Morphological, Optical, and Electronic Consequences of Coexisting Crystal Orientations in β-Copper Phthalocyanine Thin Films. Journal of Physical Chemistry C, 2016, 120, 18616-18621.	1.5	15
211	Morphology changes upon scaling a high-efficiency, solution-processed solar cell. Energy and Environmental Science, 2016, 9, 2835-2846.	15.6	170
212	A Vinyleneâ€Bridged Perylenediimideâ€Based Polymeric Acceptor Enabling Efficient Allâ€Polymer Solar Cells Processed under Ambient Conditions. Advanced Materials, 2016, 28, 8483-8489.	11.1	222
213	A PCBM Electron Transport Layer Containing Small Amounts of Dual Polymer Additives that Enables Enhanced Perovskite Solar Cell Performance. Advanced Science, 2016, 3, 1500353.	5.6	67
214	Intrinsic Charge Trapping Observed as Surface Potential Variations in diF-TES-ADT Films. ACS Applied Materials & Interfaces, 2016, 8, 21490-21496.	4.0	2
215	High efficiency and stability small molecule solar cells developed by bulk microstructure fine-tuning. Nano Energy, 2016, 28, 241-249.	8.2	57
216	Manipulation of Domain Purity and Orientational Ordering in High Performance All-Polymer Solar Cells. Chemistry of Materials, 2016, 28, 6178-6185.	3.2	87

#	Article	IF	CITATIONS
217	Controlling additive behavior to reveal an alternative morphology formation mechanism in polymer : fullerene bulk-heterojunctions. Journal of Materials Chemistry A, 2016, 4, 16136-16147.	5.2	22
218	Coulomb Enhanced Charge Transport in Semicrystalline Polymer Semiconductors. Advanced Functional Materials, 2016, 26, 8011-8022.	7.8	24
219	Designing ternary blend bulk heterojunction solar cells with reduced carrier recombination and a fill factor of 77%. Nature Energy, 2016, 1, .	19.8	330
220	Fast charge separation in a non-fullerene organic solar cell with a small driving force. Nature Energy, 2016, 1, .	19.8	1,167
221	Role of Solution Structure in Self-Assembly of Conjugated Block Copolymer Thin Films. Macromolecules, 2016, 49, 8187-8197.	2.2	18
222	Efficient organic solar cells processed from hydrocarbon solvents. Nature Energy, 2016, 1, .	19.8	2,129
223	Rigidifying Nonplanar Perylene Diimides by Ring Fusion Toward Geometryâ€Tunable Acceptors for Highâ€Performance Fullereneâ€Free Solar Cells. Advanced Materials, 2016, 28, 951-958.	11.1	238
224	A Difluorobenzoxadiazole Building Block for Efficient Polymer Solar Cells. Advanced Materials, 2016, 28, 1868-1873.	11.1	125
225	Highly Efficient Organic Solar Cells with Improved Vertical Donor–Acceptor Compositional Gradient Via an Inverted Offâ€Center Spinning Method. Advanced Materials, 2016, 28, 967-974.	11.1	256
226	Timeâ€Dependent Morphology Evolution of Solutionâ€Processed Small Molecule Solar Cells during Solvent Vapor Annealing. Advanced Energy Materials, 2016, 6, 1502579.	10.2	96
227	Influence of fluorination on the properties and performance of isoindigo–quaterthiophene-based polymers. Journal of Materials Chemistry A, 2016, 4, 5039-5043.	5.2	35
228	Comparative Photovoltaic Study of Physical Blending of Two Donor–Acceptor Polymers with the Chemical Blending of the Respective Moieties. Macromolecules, 2016, 49, 2533-2540.	2.2	31
229	Growth of thermally stable crystalline C ₆₀ films on flat-lying copper phthalocyanine. Journal of Materials Chemistry A, 2016, 4, 1028-1032.	5.2	2
230	Origins of polarization-dependent anisotropic X-ray scattering from organic thin films. Journal of Synchrotron Radiation, 2016, 23, 219-227.	1.0	26
231	Morphology Changes Upon Scaling a High-Efficiency, Solution-Processed Solar Cell From Spin-Coating to Roll-to-Roll Coating. Energy and Environmental Science, 2016, 9, .	15.6	4
232	Organic Solar Cells: Influence of Processing Parameters and Molecular Weight on the Morphology and Properties of High-Performance PffBT4T-2OD:PC71BM Organic Solar Cells (Adv. Energy Mater.) Tj ETQq0 0 C) rgBT2/Ove	erl o ck 10 Tf 5
233	Thin Films: Tuning Local Molecular Orientation-Composition Correlations in Binary Organic Thin Films by Solution Shearing (Adv. Funct. Mater. 21/2015). Advanced Functional Materials, 2015, 25, 3106-3106.	7.8	0
00.4	Significance of Average Domain Purity and Mixed Domains on the Photovoltaic Performance of	10.0	100

234 Highâ€Efficiency Solutionâ€Processed Smallâ€Molecule BHJ Solar Cells. Advanced Energy Materials, 2015, 5, 10.2 133 1500877.

#	Article	IF	CITATIONS
235	Influence of Processing Parameters and Molecular Weight on the Morphology and Properties of Highâ€Performance PffBT4Tâ€2OD:PC ₇₁ BM Organic Solar Cells. Advanced Energy Materials, 2015, 5, 1501400.	10.2	166
236	A Largeâ€Bandgap Conjugated Polymer for Versatile Photovoltaic Applications with High Performance. Advanced Materials, 2015, 27, 4655-4660.	11.1	882
237	Highâ€Performance Nonâ€Fullerene Polymer Solar Cells Based on a Pair of Donor–Acceptor Materials with Complementary Absorption Properties. Advanced Materials, 2015, 27, 7299-7304.	11.1	230
238	Manipulating Aggregation and Molecular Orientation in Allâ€Polymer Photovoltaic Cells. Advanced Materials, 2015, 27, 6046-6054.	11.1	264
239	Characterizing morphology in organic systems with resonant soft X-ray scattering. Journal of Electron Spectroscopy and Related Phenomena, 2015, 200, 2-14.	0.8	58
240	Tuning Open-Circuit Voltage in Organic Solar Cells with Molecular Orientation. ACS Applied Materials & Interfaces, 2015, 7, 13208-13216.	4.0	64
241	Influence of Regio- and Chemoselectivity on the Properties of Fluoro-Substituted Thienothiophene and Benzodithiophene Copolymers. Journal of the American Chemical Society, 2015, 137, 7616-7619.	6.6	89
242	Tuning Local Molecular Orientation–Composition Correlations in Binary Organic Thin Films by Solution Shearing. Advanced Functional Materials, 2015, 25, 3131-3137.	7.8	29
243	Dramatic performance enhancement for large bandgap thick-film polymer solar cells introduced by a difluorinated donor unit. Nano Energy, 2015, 15, 607-615.	8.2	93
244	Disruption of Molecular Ordering over Several Layers near the Au/2,8-Difluoro-5,11-bis(triethylsilylethynyl) Anthradithiophene Interface. Crystal Growth and Design, 2015, 15, 822-828.	1.4	3
245	2D-Conjugated Benzodithiophene-Based Polymer Acceptor: Design, Synthesis, Nanomorphology, and Photovoltaic Performance. Macromolecules, 2015, 48, 7156-7163.	2.2	70
246	Direct Optical Observation of Stimulated Emission from Hot Charge Transfer Excitons in Bulk Heterojunction Polymer Solar Cells. Journal of Physical Chemistry C, 2015, 119, 19697-19702.	1.5	2
247	The influence of spacer units on molecular properties and solar cell performance of non-fullerene acceptors. Journal of Materials Chemistry A, 2015, 3, 20108-20112.	5.2	41
248	Importance of Domain Purity and Molecular Packing in Efficient Solutionâ€Processed Smallâ€Molecule Solar Cells. Advanced Materials, 2015, 27, 1105-1111.	11.1	160
249	Topographic measurement of buried thin-film interfaces using a grazing resonant soft x-ray scattering technique. Physical Review B, 2014, 90, .	1.1	15
250	Interplay of Solvent Additive Concentration and Active Layer Thickness on the Performance of Small Molecule Solar Cells. Advanced Materials, 2014, 26, 7308-7316.	11.1	47
251	Correlating domain purity with charge carrier mobility in bulk heterojunction polymer solar cells. Proceedings of SPIE, 2014, , .	0.8	5
252	Controlling Molecular Weight of a High Efficiency Donorâ€Acceptor Conjugated Polymer and Understanding Its Significant Impact on Photovoltaic Properties. Advanced Materials, 2014, 26, 4456-4462.	11.1	190

#	Article	IF	CITATIONS
253	Highâ€Molecularâ€Weight Insulating Polymers Can Improve the Performance of Molecular Solar Cells. Advanced Materials, 2014, 26, 4168-4172.	11.1	101
254	The influence of molecular orientation on organic bulk heterojunction solar cells. Nature Photonics, 2014, 8, 385-391.	15.6	439
255	Enhanced Photovoltaic Performance by Modulating Surface Composition in Bulk Heterojunction Polymer Solar Cells Based on PBDTTTâ€Câ€T/PC ₇₁ BM. Advanced Materials, 2014, 26, 4043-4049.	11.1	203
256	Quantification of Nano―and Mesoscale Phase Separation and Relation to Donor and Acceptor Quantum Efficiency, <i>J</i> _{sc} , and FF in Polymer:Fullerene Solar Cells. Advanced Materials, 2014, 26, 4234-4241.	11,1	127
257	High Performance Allâ€Polymer Solar Cell via Polymer Sideâ€Chain Engineering. Advanced Materials, 2014, 26, 3767-3772.	11.1	320
258	Understanding the Morphology of PTB7:PCBM Blends in Organic Photovoltaics. Advanced Energy Materials, 2014, 4, 1301377.	10.2	203
259	On the Efficiency of Charge Transfer State Splitting in Polymer:Fullerene Solar Cells. Advanced Materials, 2014, 26, 2533-2539.	11.1	106
260	Organic Solar Cells: On the Efficiency of Charge Transfer State Splitting in Polymer:Fullerene Solar Cells (Adv. Mater. 16/2014). Advanced Materials, 2014, 26, 2607-2607.	11.1	0
261	Correlated Donor/Acceptor Crystal Orientation Controls Photocurrent Generation in Allâ€Polymer Solar Cells. Advanced Functional Materials, 2014, 24, 4068-4081.	7.8	144
262	The Role of Regioregularity, Crystallinity, and Chain Orientation on Electron Transport in a High-Mobility n-Type Copolymer. Journal of the American Chemical Society, 2014, 136, 4245-4256.	6.6	226
263	Highâ€Efficiency Allâ€Polymer Solar Cells Based on a Pair of Crystalline Lowâ€Bandgap Polymers. Advanced Materials, 2014, 26, 7224-7230.	11.1	228
264	Aggregation and morphology control enables multiple cases of high-efficiency polymer solar cells. Nature Communications, 2014, 5, 5293.	5.8	2,854
265	Toward Single-Crystal Hybrid-Carbon Electronics: Impact of Graphene Substrate Defect Density on Copper Phthalocyanine Film Growth. Crystal Growth and Design, 2014, 14, 4394-4401.	1.4	7
266	Photovoltaics: Quantification of Nano―and Mesoscale Phase Separation and Relation to Donor and Acceptor Quantum Efficiency, <i>J</i> _{sc} , and FF in Polymer:Fullerene Solar Cells (Adv.) Tj ETQq0 0 C) rgBTi/Ov	erløck 10 Tf 5
267	Fullerene-Free Polymer Solar Cells with Highly Reduced Bimolecular Recombination and Field-Independent Charge Carrier Generation. Journal of Physical Chemistry Letters, 2014, 5, 2815-2822.	2.1	42
268	A Polythiophene Derivative with Superior Properties for Practical Application in Polymer Solar Cells. Advanced Materials, 2014, 26, 5880-5885.	11.1	205
269	Mobility-Controlled Performance of Thick Solar Cells Based on Fluorinated Copolymers. Journal of the American Chemical Society, 2014, 136, 15566-15576.	6.6	249
270	Morphology linked to miscibility in highly amorphous semi-conducting polymer/fullerene blends. Polymer, 2014, 55, 4884-4889.	1.8	32

#	Article	IF	CITATIONS
271	Influence of Fluorination and Molecular Weight on the Morphology and Performance of PTB7:PC ₇₁ BM Solar Cells. Journal of Physical Chemistry C, 2014, 118, 9918-9929.	1.5	43
272	Quantifying Charge Extraction in Organic Solar Cells: The Case of Fluorinated PCPDTBT. Journal of Physical Chemistry Letters, 2014, 5, 1131-1138.	2.1	88
273	An Easy and Effective Method to Modulate Molecular Energy Level of the Polymer Based on Benzodithiophene for the Application in Polymer Solar Cells. Advanced Materials, 2014, 26, 2089-2095.	11.1	137
274	Competition between morphological attributes in the thermal annealing and additive processing of polymer solar cells. Journal of Materials Chemistry C, 2013, 1, 5023.	2.7	44
275	On the role of intermixed phases in organic photovoltaic blends. Energy and Environmental Science, 2013, 6, 2756.	15.6	157
276	Organic Solar Cells: Domain Purity, Miscibility, and Molecular Orientation at Donor/Acceptor Interfaces in High Performance Organic Solar Cells: Paths to Further Improvement (Adv. Energy) Tj ETQq0 0 0 rgE	BT 10 værloo	ck 110 Tf 50 5
277	Modifications in Morphology Resulting from Nanoimprinting Bulk Heterojunction Blends for Light Trapping Organic Solar Cell Designs. ACS Applied Materials & Interfaces, 2013, 5, 8225-8230.	4.0	8
278	Fluorinated Polymer Yields High Organic Solar Cell Performance for a Wide Range of Morphologies. Advanced Functional Materials, 2013, 23, 3463-3470.	7.8	91
279	Absolute Measurement of Domain Composition and Nanoscale Size Distribution Explains Performance in PTB7:PC ₇₁ BM Solar Cells. Advanced Energy Materials, 2013, 3, 65-74.	10.2	605
280	Differences in NEXAFS of odd/even long chain n-alkane crystals. Journal of Electron Spectroscopy and Related Phenomena, 2013, 191, 60-64.	0.8	6
281	Soft X-ray characterisation of organic semiconductor films. Journal of Materials Chemistry C, 2013, 1, 187-201.	2.7	75
282	Domain Purity, Miscibility, and Molecular Orientation at Donor/Acceptor Interfaces in High Performance Organic Solar Cells: Paths to Further Improvement. Advanced Energy Materials, 2013, 3, 864-872.	10.2	283
283	Fluorine Substituents Reduce Charge Recombination and Drive Structure and Morphology Development in Polymer Solar Cells. Journal of the American Chemical Society, 2013, 135, 1806-1815.	6.6	528
284	PDTâ€Sâ€T: A New Polymer with Optimized Molecular Conformation for Controlled Aggregation and <i>ï€</i> – <i>ï€</i> Stacking and Its Application in Efficient Photovoltaic Devices. Advanced Materials, 2013, 25, 3449-3455.	11.1	190
285	Molecular Design toward Efficient Polymer Solar Cells with High Polymer Content. Journal of the American Chemical Society, 2013, 135, 8464-8467.	6.6	86
286	The Importance of Fullerene Percolation in the Mixed Regions of Polymer–Fullerene Bulk Heterojunction Solar Cells. Advanced Energy Materials, 2013, 3, 364-374.	10.2	412
287	Disentangling the impact of side chains and fluorine substituents of conjugated donor polymers on the performance of photovoltaic blends. Energy and Environmental Science, 2013, 6, 316-326.	15.6	153
288	Thermally Induced Dewetting in Ultrathin C ₆₀ Films on Copper Phthalocyanine. Journal of Physical Chemistry C, 2013, 117, 26007-26012.	1.5	3

#	Article	IF	CITATIONS
289	Synthesis, solidâ€state, and chargeâ€transport properties of conjugated polythiopheneâ€ <i>S</i> , <i>S</i> â€dioxides. Journal of Polymer Science, Part B: Polymer Physics, 2013, 51, 48-56.	2.4	22
290	Accurate and Facile Determination of the Index of Refraction of Organic Thin Films Near the Carbon <mml:math <br="" xmlns:mml="http://www.w3.org/1998/Math/MathML">display="inline"><mml:mn>1</mml:mn><mml:mi>s</mml:mi></mml:math> Absorption Edge. Physical Review Letters, 2013, 110, 177401.	2.9	42
291	Influence of dielectric-dependent interfacial widths on device performance in top-gate P(NDI2OD-T2) field-effect transistors. Applied Physics Letters, 2012, 101, 093308.	1.5	18
292	2011 ALS User Meeting and Workshops. Synchrotron Radiation News, 2012, 25, 4-8.	0.2	0
293	Soft X-ray Imaging of Polymers and Polymer Composites. Microscopy and Microanalysis, 2012, 18, 1612-1613.	0.2	0
294	Correlating the Efficiency and Nanomorphology of Polymer Blend Solar Cells Utilizing Resonant Soft X-ray Scattering. ACS Nano, 2012, 6, 677-688.	7.3	149
295	Quantitative compositional analysis of organic thin films using transmission NEXAFS spectroscopy in an X-ray microscope. Journal of Electron Spectroscopy and Related Phenomena, 2012, 185, 119-128.	0.8	64
296	From Binary to Ternary Solvent: Morphology Fineâ€ŧuning of D/A Blends in PDPP3Tâ€based Polymer Solar Cells. Advanced Materials, 2012, 24, 6335-6341.	11.1	288
297	Engineering biodegradable polymer blends containing flame retardant-coated starch/nanoparticles. Polymer, 2012, 53, 4787-4799.	1.8	35
298	Studying Polymer/Fullerene Intermixing and Miscibility in Laterally Patterned Films with Xâ€Ray Spectromicroscopy. Small, 2012, 8, 1920-1927.	5.2	39
299	Polarized X-ray scattering reveals non-crystalline orientational ordering in organic films. Nature Materials, 2012, 11, 536-543.	13.3	281
300	NEXAFS imaging of synthetic organic materials. Materials Today, 2012, 15, 148-157.	8.3	50
301	Fullerene-Dependent Miscibility in the Silole-Containing Copolymer PSBTBT-08. Macromolecules, 2011, 44, 9747-9751.	2.2	59
302	Miscibility, Crystallinity, and Phase Development in P3HT/PCBM Solar Cells: Toward an Enlightened Understanding of Device Morphology and Stability. Journal of Physical Chemistry Letters, 2011, 2, 3135-3145.	2.1	301
303	Defining the Nanostructured Morphology of Triblock Copolymers Using Resonant Soft X-ray Scattering. Nano Letters, 2011, 11, 3906-3911.	4.5	139
304	The use of functionalized nanoparticles as nonâ€ s pecific compatibilizers for polymer blends. Polymers for Advanced Technologies, 2011, 22, 65-71.	1.6	28
305	Interfaces in organic devices studied with resonant soft x-ray reflectivity. Journal of Applied Physics, 2011, 110, .	1.1	27
306	The case for soft X-rays: Improved compositional contrast for structure and morphology determination with real and reciprocal space methods. IOP Conference Series: Materials Science and Engineering, 2010, 14, 012020.	0.3	6

#	Article	IF	CITATIONS
307	Quantitative Soft X-ray Microscopy of Soft Matter. Microscopy and Microanalysis, 2010, 16, 888-889.	0.2	0
308	A new Scanning Transmission X-ray Microscope at the ALS for operation up to 2500eV. , 2010, , .		10
309	Influence of Annealing and Interfacial Roughness on the Performance of Bilayer Donor/Acceptor Polymer Photovoltaic Devices. Advanced Functional Materials, 2010, 20, 4329-4337.	7.8	105
310	Improved efficiency of bulk heterojunction poly(3-hexylthiophene):[6,6]-phenyl-C61-butyric acid methyl ester photovoltaic devices using discotic liquid crystal additives. Applied Physics Letters, 2010, 96, 183305.	1.5	54
311	Interfacial Interactions in PP/MMT/SEBS Nanocomposites. Macromolecules, 2010, 43, 448-453.	2.2	44
312	Probing the Chain and Crystal Lattice Orientation in Polyethylene Thin Films by Near Edge X-ray Absorption Fine Structure (NEXAFS) Spectroscopy. Macromolecules, 2010, 43, 8153-8161.	2.2	13
313	Nanomorphology of Bulk Heterojunction Photovoltaic Thin Films Probed with Resonant Soft X-ray Scattering. Nano Letters, 2010, 10, 2863-2869.	4.5	182
314	Molecular Miscibility of Polymerâ^'Fullerene Blends. Journal of Physical Chemistry Letters, 2010, 1, 3160-3166.	2.1	362
315	The effect of angle of incidence on the optical field distribution within thin film organic solar cells. Journal of Applied Physics, 2009, 106, .	1.1	32
316	Characterization of multicomponent polymer trilayers with resonant soft Xâ€ray reflectivity. Journal of Polymer Science, Part B: Polymer Physics, 2009, 47, 1291-1299.	2.4	24
317	Near-edge X-ray absorption fine-structure microscopy of organic and magnetic materials. Nature Materials, 2009, 8, 281-290.	13.3	141
318	Spectromicroscopy Study of Intercalation and Exfoliation in Polypropylene/Montmorillonite Nanocomposites. Journal of Physical Chemistry B, 2009, 113, 11160-11165.	1.2	30
319	Evolution of Laterally Phase-Separated Polyfluorene Blend Morphology Studied by X-ray Spectromicroscopy. Macromolecules, 2009, 42, 3347-3352.	2.2	43
320	Interfacial Widths of Conjugated Polymer Bilayers. Journal of the American Chemical Society, 2009, 131, 12538-12539.	6.6	42
321	First Direct Imaging of Electrolyte-Induced Deswelling Behavior of pH-Responsive Microgels in Aqueous Media Using Scanning Transmission X-ray Microscopy. Langmuir, 2009, 25, 2588-2592.	1.6	37
322	A Quantitative Study of PCBM Diffusion during Annealing of P3HT:PCBM Blend Films. Macromolecules, 2009, 42, 8392-8397.	2.2	247
323	Role of Solvent Trapping Effects in Determining the Structure and Morphology of Ternary Blend Organic Devices. Macromolecules, 2009, 42, 3098-3103.	2.2	42
324	NEXAFS microscopy and resonant scattering: Composition and orientation probed in real and reciprocal space. Polymer, 2008, 49, 643-675.	1.8	261

#	Article	IF	CITATIONS
325	A simple method for determining linear polarization and energy calibration of focused soft X-ray beams. Journal of Electron Spectroscopy and Related Phenomena, 2008, 162, 49-55.	0.8	56
326	Organic thermometry for chondritic parent bodies. Earth and Planetary Science Letters, 2008, 272, 446-455.	1.8	204
327	Quantitative organic and lightâ€element analysis of comet 81P/Wild 2 particles using Câ€, Nâ€, and Oâ€Ĥ⁄4â€XAI Meteoritics and Planetary Science, 2008, 43, 353-365.	NES. 0.7	137
328	Evolution of the nanomorphology of photovoltaic polyfluorene blends: sub-100 nm resolution with x-ray spectromicroscopy. Nanotechnology, 2008, 19, 424015.	1.3	47
329	PolLux: A new facility for soft x-ray spectromicroscopy at the Swiss Light Source. Review of Scientific Instruments, 2008, 79, 113704.	0.6	222
330	X-ray Microscopy of Soft Matter. Microscopy and Microanalysis, 2008, 14, 58-59.	0.2	0
331	Mass fractionation of carbon and hydrogen secondary ions upon Cs+ and O2+ bombardment of organic materials. Journal of Vacuum Science and Technology A: Vacuum, Surfaces and Films, 2007, 25, 480-484.	0.9	2
332	Resonant soft x-ray reflectivity of organic thin films. Journal of Vacuum Science and Technology A: Vacuum, Surfaces and Films, 2007, 25, 575-586.	0.9	67
333	Carbon-13 Labeling for Quantitative Analysis of Molecular Movement in Heterogeneous Organic Materials Using Secondary Ion Mass Spectrometry. Analytical Chemistry, 2007, 79, 5358-5363.	3.2	4
334	X-ray Microscopy of Photovoltaic Polyfluorene Blends:Â Relating Nanomorphology to Device Performance. Macromolecules, 2007, 40, 3263-3270.	2.2	102
335	Influence of sample preparation and processing on observed glass transition temperatures of polymer nanocomposites. Journal of Polymer Science, Part B: Polymer Physics, 2007, 45, 2270-2276.	2.4	28
336	Solid state effects in the NEXAFS spectra of alkane-based van der Waals crystals: Breakdown of molecular model. Chemical Physics Letters, 2006, 430, 287-292.	1.2	23
337	Compatibilizing Bulk Polymer Blends by Using Organoclays. Macromolecules, 2006, 39, 4793-4801.	2.2	316
338	Polystyrene/Poly(methyl methacrylate) Blends in the Presence of Cyclohexane:Â Selective Solvent Washing or Equilibrium Adsorption?. Macromolecules, 2006, 39, 7729-7733.	2.2	16
339	Investigation of the Effects of Isotopic Labeling at a PS/PMMA Interface Using SIMS and Mean-Field Theory. Macromolecules, 2006, 39, 1639-1645.	2.2	18
340	Carbon-13 Labeled Polymers:  An Alternative Tracer for Depth Profiling of Polymer Films and Multilayers Using Secondary Ion Mass Spectrometry. Analytical Chemistry, 2006, 78, 3452-3460.	3.2	7
341	Changes in Thermodynamic Interactions at Highly Immiscible Polymer/Polymer Interfaces due to Deuterium Labeling. Journal of Physical Chemistry B, 2006, 110, 10602-10605.	1.2	11
342	Direct spincasting of polystyrene thin films onto poly(methyl methacrylate). Journal of Polymer Science, Part B: Polymer Physics, 2006, 44, 3234-3244.	2.4	29

#	Article	IF	CITATIONS
343	SIMS depth profiling of deuterium labeled polymers in polymer multilayers. Applied Surface Science, 2006, 252, 7224-7227.	3.1	4
344	Carbon-13 labeling for improved tracer depth profiling of organic materials using secondary ion mass spectrometry. Journal of the American Society for Mass Spectrometry, 2006, 17, 1142-1145.	1.2	11
345	Resonant soft x-ray scattering from structured polymer nanoparticles. Applied Physics Letters, 2006, 89, 124106.	1.5	66
346	Low-temperature reactive coupling at polymer–polymer interfaces facilitated by supercritical CO2. Polymer, 2005, 46, 10173-10179.	1.8	15
347	Conduction band states of transition metal (TM) high-k gate dielectrics as determined from X-ray absorption spectra. Microelectronics Reliability, 2005, 45, 827-830.	0.9	2
348	Soft x-ray resonant reflectivity of low-Z material thin films. Applied Physics Letters, 2005, 87, 214109.	1.5	103
349	Conduction band-edge States associated with the removal of d-state degeneracies by the Jahn-Teller effect. IEEE Transactions on Device and Materials Reliability, 2005, 5, 65-83.	1.5	63
350	Direct Imaging and Spectroscopic Characterization of Stimulus-Responsive Microgels. Journal of the American Chemical Society, 2005, 127, 16808-16809.	6.6	48
351	Diffusion-Controlled Reactive Coupling at Polymerâ^'Polymer Interfaces. Macromolecules, 2005, 38, 3543-3546.	2.2	35
352	Investigation of Blend Miscibility of a Ternary PS/PCHMA/PMMA System Using SIMS and Mean-Field Theory. Macromolecules, 2005, 38, 10511-10515.	2.2	11
353	Shape stability of TiSi2 islands on Si (111). Journal of Applied Physics, 2004, 95, 1572-1576.	1.1	21
354	Spectroscopic studies of metal high-k dielectrics: transition metal oxides and silicates, and complex rare earth/transition metal oxides. Physica Status Solidi (B): Basic Research, 2004, 241, 2221-2235.	0.7	27
355	Crystallization in the Thin and Ultrathin Films of Poly(ethyleneâ~'vinyl acetate) and Linear Low-Density Polyethylene. Macromolecules, 2004, 37, 3319-3327.	2.2	139
356	X-ray Linear Dichroism Microscopy of Crystalline Short Chain Alkanes and Semi-crystalline Polyethylene Thin Films. Microscopy and Microanalysis, 2004, 10, 1020-1021.	0.2	2
357	Scanning Transmission X-ray Microscopes at the Advanced Light Source: Performance and Experimental Capabilities. Microscopy and Microanalysis, 2004, 10, 1018-1019.	0.2	3
358	Orientation studies of Si-phthalocyanine sulfonic acids cast on SiO x substrates. Applied Physics A: Materials Science and Processing, 2003, 76, 177-182.	1.1	3
359	Towards a detailed understanding of the NEXAFS spectra of bulk polyethylene copolymers and related alkanes. Chemical Physics Letters, 2003, 370, 834-841.	1.2	67
360	Electronic structure of transition metal high-k dielectrics: interfacial band offset energies for microelectronic devices. Applied Surface Science, 2003, 212-213, 563-569.	3.1	21

#	Article	IF	CITATIONS
361	Calibrated NEXAFS spectra of some common polymers. Journal of Electron Spectroscopy and Related Phenomena, 2003, 128, 85-96.	0.8	249
362	Interferometer-controlled scanning transmission X-ray microscopes at the Advanced Light Source. Journal of Synchrotron Radiation, 2003, 10, 125-136.	1.0	625
363	Use of functionalized WS2 nanotubes to produce new polystyrene/polymethylmethacrylate nanocomposites. Polymer, 2003, 44, 2109-2115.	1.8	43
364	Attractive Migration and Coalescence: A Significant Process in the Coarsening ofTiSi2Islands on the Si(111) Surface. Physical Review Letters, 2003, 90, 136102.	2.9	47
365	Soft Xâ€ray Microcopy at the ALS. Synchrotron Radiation News, 2003, 16, 16-27.	0.2	3
366	Surface Morphology of Annealed Polystyrene and Poly(methyl methacrylate) Thin Film Blends and Bilayers. Macromolecules, 2003, 36, 3307-3314.	2.2	101
367	Tuning Substrate Surface Energies for Blends of Polystyrene and Poly(methyl methacrylate). Langmuir, 2003, 19, 8526-8535.	1.6	25
368	Application of Scanning Transmission X-Ray Microscopy to the Rubber Industry. Rubber Chemistry and Technology, 2003, 76, 803-811.	0.6	5
369	Trends in the Carbonyl Core (C 1S, O 1S) → ï€*C=O Transition in the Near-Edge X-ray Absorption Fine Structure Spectra of Organic Molecules. Journal of Physical Chemistry B, 2002, 106, 8531-8538.	1.2	271
370	NEXAFS SPECTROSCOPY AND MICROSCOPY OF NATURAL AND SYNTHETIC POLYMERS. Advanced Series in Physical Chemistry, 2002, , 285-355.	1.5	45
371	Identification and Quantitation of Urea Precipitates in Flexible Polyurethane Foam Formulations by X-ray Spectromicroscopy. Macromolecules, 2002, 35, 5873-5882.	2.2	69
372	Effect of Methyl Methacrylate/Polyhedral Oligomeric Silsesquioxane Random Copolymers in Compatibilization of Polystyrene and Poly(methyl methacrylate) Blends. Macromolecules, 2002, 35, 8029-8038.	2.2	120
373	Quantitative Characterization of Microscopic Variations in the Cross-Link Density of Gels. Macromolecules, 2002, 35, 1336-1341.	2.2	44
374	A new bend-magnet beamline for scanning transmission X-ray microscopy at the Advanced Light Source. Journal of Synchrotron Radiation, 2002, 9, 254-257.	1.0	120
375	Characterization of the effects of soft X-ray irradiation on polymers. Journal of Electron Spectroscopy and Related Phenomena, 2002, 122, 65-78.	0.8	186
376	Anomalous Phase Inversion in Polymer Blends Prepared by Cryogenic Mechanical Alloying. Macromolecules, 2001, 34, 1536-1538.	2.2	30
377	Effect of Carbon Black and Silica Fillers in Elastomer Blends. Macromolecules, 2001, 34, 7056-7065.	2.2	83
378	Use of near Edge X-Ray Absorption Fine Structure Spectromicroscopy to Characterize Multicomponent Polymeric Systems. Applied Spectroscopy, 2001, 55, 1676-1681.	1.2	14

Harald Ade

#	Article	IF	CITATIONS
379	X-ray spectromicroscopy of immiscible polymer blends: polystyrene–poly(methyl methacrylate). Journal of Electron Spectroscopy and Related Phenomena, 2001, 121, 203-224.	0.8	62
380	Optimization of scanning transmission X-ray microscopy for the identification and quantitation of reinforcing particles in polyurethanes. Ultramicroscopy, 2001, 88, 33-49.	0.8	31
381	Cryogenic mechanical alloying as an alternative strategy for the recycling of tires. Polymer, 2001, 42, 4453-4457.	1.8	41
382	Interfacial properties of elastomer blends as studied by neutron reflectivity. Polymer, 2001, 42, 9133-9141.	1.8	5
383	On the similarity of macromolecular responses to high-energy processes: mechanical milling vs. irradiation. Polymer Degradation and Stability, 2001, 72, 519-524.	2.7	19
384	Near-edge X-ray absorption fine structure (NEXAFS) microscopy of a polycarbonate/poly(acrylonitrile/butadiene/styrene) blend. Journal of Polymer Science, Part B: Polymer Physics, 2001, 39, 531-535.	2.4	8
385	Electronic structure of noncrystalline transition metal silicate and aluminate alloys. Applied Physics Letters, 2001, 79, 1775-1777.	1.5	66
386	Solid-State Blending of Polymers by Cryogenic Mechanical Alloying. Materials Research Society Symposia Proceedings, 2000, 629, 1.	0.1	10
387	Temperature-induced morphological evolution in polymer blends produced by cryogenic mechanical alloying. Macromolecular Materials and Engineering, 2000, 274, 1-12.	1.7	20
388	Substrate dependence of morphology in thin film polymer blends of polystyrene and poly(methyl) Tj ETQq0 0 0 r	gBT /Overl 1.6	ock 10 Tf 50
389	Chemical and vibronic effects in the high-resolution near-edge X-ray absorption fine structure spectra of polystyrene isotopomers. Chemical Physics Letters, 2000, 322, 412-418.	1.2	37
390	Illumination for coherent soft X-ray applications: the new X1A beamline at the NSLS. Journal of Synchrotron Radiation, 2000, 7, 395-404.	1.0	54
391	High-energy mechanical milling of poly(methyl methacrylate), polyisoprene and poly(ethylene- alt) Tj ETQq1 1 0.7	784314 rg 1.8	BT/Overlock
392	Time–Temperature Superposition of Phase Separating Polymer Blend Films. High Performance Polymers, 2000, 12, 599-602.	0.8	8
393	Addition of a Block Copolymer to Polymer Blends Produced by Cryogenic Mechanical Alloying. Macromolecules, 2000, 33, 1163-1172.	2.2	38
394	Effect of an Interactive Surface on the Equilibrium Contact Angles in Bilayer Polymer Films. Langmuir, 2000, 16, 2369-2375.	1.6	53
395	Cryogenic Mechanical Alloying of Poly(methyl methacrylate) with Polyisoprene and Poly(ethylene-alt-propylene). Macromolecules, 2000, 33, 2595-2604.	2.2	49
396	X-RAY SPECTROMICROSCOPY. , 1999, , 225-262.		6

#	Article	IF	CITATIONS
397	Phase segregation in polymer thin films: Elucidations by X-ray and scanning force microscopy. Europhysics Letters, 1999, 45, 526-532.	0.7	62
398	NEXAFS spectromicroscopy of polymers: overview and quantitative analysis of polyurethane polymers. Journal of Electron Spectroscopy and Related Phenomena, 1999, 100, 119-135.	0.8	101
399	Imaging electron emission from diamond and Ill–V nitride surfaces with photo-electron emission microscopy. Applied Surface Science, 1999, 146, 287-294.	3.1	11
400	High-Energy Cryogenic Blending and Compatibilizing of Immiscible Polymers. Advanced Materials, 1999, 11, 1277-1281.	11.1	48
401	Near-Edge X-ray Absorption Fine Structure Spectroscopy of MDI and TDI Polyurethane Polymers. Journal of Physical Chemistry B, 1999, 103, 4603-4610.	1.2	50
402	Near-Edge X-ray Absorption Fine Structure Spectroscopy on Ordered Films of an Amphiphilic Derivate of 2,5-Diphenyl-1,3,4-Oxadiazole. Langmuir, 1999, 15, 1291-1298.	1.6	31
403	Development of scanning X-ray microscopes for materials science spectromicroscopy at the Advanced Light Source. Journal of Synchrotron Radiation, 1998, 5, 1090-1092.	1.0	27
404	Determination of chemical-structural changes in vitrinite accompanying luminescence alteration using C-NEXAFS analysis. Organic Geochemistry, 1998, 28, 441-455.	0.9	104
405	Phase Separation of Polystyrene and Bromoâ^'Polystyrene Mixtures in Equilibrium Structures in Thin Films. Langmuir, 1998, 14, 4860-4864.	1.6	48
406	Bulk and surface characterization of a dewetting thin film polymer bilayer. Applied Physics Letters, 1998, 73, 3775-3777.	1.5	64
407	A scanning transmission x-ray microscope for materials science spectromicroscopy at the advanced light source. Review of Scientific Instruments, 1998, 69, 2964-2973.	0.6	96
408	11. X-Ray Spectromicroscopy. Experimental Methods in the Physical Sciences, 1998, , 225-262.	0.1	16
409	High-Resolution X-Ray Photoemission Electron Microscopy at the Advanced Light Source. Materials Research Society Symposia Proceedings, 1998, 524, 25.	0.1	1
410	Spectromicroscopy of Poly(ethylene terephthalate):  Comparison of Spectra and Radiation Damage Rates in X-ray Absorption and Electron Energy Loss. Journal of Physical Chemistry B, 1997, 101, 1950-1960.	1.2	187
411	Inner-Shell Excitation Spectroscopy of Polymer and Monomer Isomers of Dimethyl Phthalate. Journal of Physical Chemistry B, 1997, 101, 2267-2276.	1.2	65
412	X-ray Microscopy and NEXAFS Spectroscopy of Macrophase-Separated Random Block Copolymer/Homopolymer Blends. Macromolecules, 1997, 30, 663-666.	2.2	12
413	X-ray spectromicroscopy of polymers and tribological surfaces at beamline X1A at the NSLS. Journal of Electron Spectroscopy and Related Phenomena, 1997, 84, 53-72.	0.8	86
414	Soft X-ray spectromicroscopy development for materials science at the Advanced Light Source. Journal of Electron Spectroscopy and Related Phenomena, 1997, 84, 85-98.	0.8	45

#	Article	IF	CITATIONS
415	<title>Chemical state mapping on material surfaces with the X1A second-generation scanning photoemission microscope (X1A SPEM-II)</title> . , 1995, 2516, 150.		4
416	Development of a second generation scanning photoemission microscope with a zone plate generated microprobe at the National Synchrotron Light Source. Review of Scientific Instruments, 1995, 66, 1416-1418.	0.6	34
417	Instrumentation developments in scanning soft xâ€ray microscopy at the NSLS (invited). Review of Scientific Instruments, 1995, 66, 1271-1275.	0.6	24
418	Inner-Shell Spectroscopy and Imaging of a Subbituminous Coal: In-Situ Analysis of Organic and Inorganic Microstructure Using C(1s)-, Ca(2p)-, and Cl(2s)-NEXAFS. Energy & Fuels, 1995, 9, 525-533.	2.5	77
419	C-NEXAFS Microanalysis and Scanning X-ray Microscopy of Microheterogeneities in a High-Volatile A Bituminous Coal. Energy & Fuels, 1995, 9, 75-83.	2.5	22
420	Selective chemical mapping of coal microheterogeneity by scanning transmission x-ray microscopy. Energy & Fuels, 1994, 8, 151-154.	2.5	41
421	Nexafs microscopy of polymeric samples. Synchrotron Radiation News, 1994, 7, 11-15.	0.2	24
422	Applications of the Xia Scanning Photoemission Spectromicroscope for Element Identification on Material Surfaces. Materials Research Society Symposia Proceedings, 1994, 375, 303.	0.1	2
423	X-ray Linear Dichroism Microscopy. Science, 1993, 262, 1427-1429.	6.0	161
424	Second-generation scanning photoemission microscope at the National Synchrotron Light Source. Proceedings Annual Meeting Electron Microscopy Society of America, 1993, 51, 650-651.	0.0	0
425	Chemical contrast in X-ray microscopy and spatially resolved XANES spectroscopy of organic specimens. Science, 1992, 258, 972-975.	6.0	356
426	Scanning photoemission microscopy with synchrotron radiation. Nuclear Instruments and Methods in Physics Research, Section A: Accelerators, Spectrometers, Detectors and Associated Equipment, 1992, 319, 311-319.	0.7	24
427	X-ray Microscopy with the NSLS Soft X-ray Undulator. Physica Scripta, 1990, T31, 12-17.	1.2	8
428	The scanning transmission microscope at the NSLS. Nuclear Instruments and Methods in Physics Research, Section A: Accelerators, Spectrometers, Detectors and Associated Equipment, 1990, 291, 54-59.	0.7	25
429	Scanning photoelectron microscope with a zone plate generated microprobe. Nuclear Instruments and Methods in Physics Research, Section A: Accelerators, Spectrometers, Detectors and Associated Equipment, 1990, 291, 126-131.	0.7	36
430	A scanning photoelectron microscope (SPEM) at the NSLS. Physica Scripta, 1990, 41, 737-739.	1.2	11
431	Xâ€ray spectromicroscopy with a zone plate generated microprobe. Applied Physics Letters, 1990, 56, 1841-1843.	1.5	119

 $\label{eq:approx_state} 432 \qquad \text{A molecular interaction} \\ \hat{a} \in \texttt{``diffusion framework for predicting organic solar cell stability., 0, , .}$

96